JOURNAL OF Materials CHEMISTRY

Thermal dehydration of $H_{3+x}PV_xM_{12-x}O_{40}\cdot yH_2O$ Keggin type heteropolyacids; formation, thermal stability and structure of the anhydrous acids $H_3PM_{12}O_{40}$, of the corresponding anhydrides $PM_{12}O_{38.5}$ and of a novel trihydrate $H_3PW_{12}O_{40}\cdot 3H_2O$†

Laszlo Marosi,[a] Estrella Escalona Platero,[a] Joan Cifre[b] and Carlos Otero Areán[a]

[a]*Departamento de Química, Universidad de las Islas Baleares, 07071 Palma, Spain*
[b]*Laboratori d' Anàlisis i Assaigs, Universidad de las Islas Baleares, 07071 Palma, Spain*

Received 22nd February 2000, Accepted 17th May 2000
Published on the Web 14th July 2000

The formation and thermal stability of the catalytically important anhydrous acids $H_3PM_{12}O_{40}$ (M = Mo,W,V), of the corresponding anhydrides $PM_{12}O_{38.5}$ and of a novel first time isolated trihydrate $H_3PW_{12}O_{40}\cdot 3H_2O$ have been studied by high temperature X-ray diffraction (XRD) and thermogravimetry (TG). The corresponding crystal structures were determined from X-ray powder data using the Rietveld method and by deriving three-dimensional structure models from the experimental radial distribution functions.

The true unit cell symmetry of the anhydrous acid $H_3PMo_{12}O_{40}$ is rhombohedral, space group $R3$, $a = 11.48$ Å, $\alpha = 87.46°$, $Z = 2$. Its crystal structure is built up from distorted ($PMo_{12}O_{40}$) Keggin units. The molecular centers of the Keggin units form a rhombohedral distorted cubic body centered lattice. The structure resembles that of the cubic ammonium/potassium salts. However, due to the formation of hydrogen bridges between the polyanions, the orientation of the Keggin units is different.

Heat treatment of the anhydrous acid between 673 K and 733 K leads to the release of the constitutional water molecules with the formation of an amorphous anhydride. The anhydride structure is built up from lacunary polyions $PMo_{12}O_{38}^{+}$ and $PMo_{12}O_{39}^{-}$ in a three dimensional arrangement very similar to that of the corresponding anhydrous acid. However, the mutual orientation of the polyions is largely disordered.

Dehydration of $H_3PW_{12}O_{40}\cdot 6H_2O$ between 413 K and 453 K results in the formation of a new cubic acid containing three molecules of water of crystallization. Its structure is closely related to that of the well known hexahydrate. Both structures may be thought of as being made up of two different interpenetrating substructures of anions and cations with space group symmetry $Pn3m$. The anionic substructures are similar; the cationic substructures, however, are different. In the hexahydrate structure the polyanions are linked by nearly planar $H_5O_2^{+}$ dioxonium cations and the oxygen atoms occupy the $x, \frac{1}{4}, \frac{3}{4}$ crystallographic sites. The release of water leads to the formation of H_3O^{+} oxonium cations which occupy the regular cationic positions $\frac{1}{4}, \frac{3}{4}, \frac{3}{4}$. The molecular formula of the new trihydrate should be written as $(H_3O^{+})_3PW_{12}O_{40}$.

Introduction

Keggin type heteropolyacids (HPAs) are highly active and selective homogeneous and heterogeneous catalysts. Owing to their acidic and redox properties they are effective in both acid catalyzed and oxidation reactions. There are at least five industrial processes which utilize HPA based catalysts, among them the oxidation of methacrolein and isobutyric acid to methacrylic acid.[1,2]

Numerous studies have been carried out on the thermal stability of different HPAs and on the identification of the structures involved in catalytic reactions using XRD, TG, IR and a variety of other physical characterization techniques.[3–8] Catalytic activity was correlated with the appearance of the anhydrous acid[3,4] and, based on TG measurements, the existence of an anhydride responsible for the catalytic activity has also been postulated.[9–11]

TG on $H_3PMo_{12}O_{40}\cdot yH_2O$ (Fig. 1a) shows a rapid and nearly linear loss of the water of crystallization from 303 K to 403 K. Between 403 K and 663 K the weight on the TG pattern remains constant and the plateau in this range of temperature is ascribed to the stoichiometric anhydrous acid $H_3PMo_{12}O_{40}$. The small weight loss on TG between 673–713 K corresponds to the loss of 1.5 molecules of constitutional water. Above these temperatures the weight on TG remains constant and the state for which the solid maintains constant weight is commonly called the anhydride. There is general agreement in the literature on the assignment of the distinct steps of dehydration to the certain acid hydrates and on the accompanying structural transformations. The different products are characterized by their XRD patterns and chemical composition but there are also some points of controversy. The release of the constitutional water occurs with the formation of different

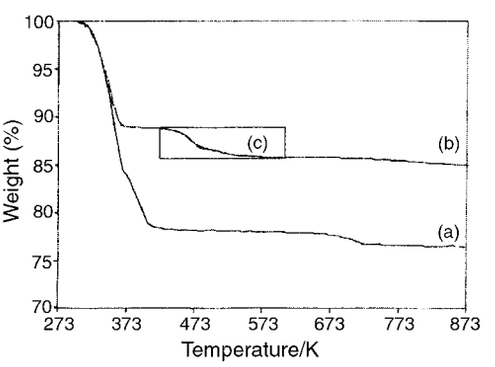

Fig. 1 TG curves of (a) $HPMo12\cdot yH_2O$, and (b) $HPW12\cdot yH_2O$.

†Present address: Leuschnerstr. 32, 67063 Ludwigshafen, Germany.

DOI: 10.1039/b001476l

This journal is © The Royal Society of Chemistry 2000

water free amorphous and crystalline phases, and reports of the nature of the anhydride phase are controversial.[3,4,9,12] The existence of an anhydride within the narrow range of temperature between 653 K and 683 K is claimed. It was concluded from IR and Raman measurements that the Keggin structure was preserved in the anhydride state.[10] However, because of the lack of detailed structural data such conclusions are not generally accepted. Some authors favor the view that the true anhydride is formed at temperatures higher than 713 K and possesses a perovskite like structure.[3,9] In order to elucidate the phase transformations over the temperature range of 653–753 K a detailed *in situ* XRD study has been performed.

Similar uncertainties exist concerning the structures of the anhydrous acids and of the corresponding anhydrides. The hydrated HPAs release the water of crystallization with the formation of dehydrated, generally poorly crystalline species for which structure determination is more difficult. Possibly because of this reason, very little crystallographic information about the structures of the catalytically active phases, *i.e.* of the anhydrous acid and of the corresponding anhydride, is available. The anhydrous acid was first indexed in the literature using tetragonal symmetry.[6] Recently, a further tetragonal cell, an orthorhombic and a hexagonal one were proposed.[4] No further crystallographic data are available about the atomic structure of this acid.

Because knowledge of structure is an important step towards understanding catalytic activity and thermal stability it seemed to us of interest to reinvestigate the HPA thermal dehydration process with special emphasis to the chemical and structural characterization of the dehydrated products containing less than six water molecules.

Methods

Materials

The $H_3PMo_{12}O_{40}\cdot yH_2O$ and $H_3PW_{12}O_{40}\cdot yH_2O$ acid hydrates were obtained from Fluka AG. The mass loss due to drying was 21–23 *m*/*m* and 14–16 *m*/*m*, respectively. According to XRD analysis the materials consisted of a mixture of different hydrates containing 29, 21 and 13 water molecules. These starting materials are referred to as HPM12·yH_2O in the following discussion.

The $H_4PVMo_{11}O_{40}$ HPA was synthesized according to the method of Tsigdinos and Hallada[13] by acidification of an aqueous solution of sodium phosphate, molybdate, and vanadate with concentrated sulfuric acid followed by extraction with diethylene oxide. After separation the ether was evaporated off. The orange solid that remained was dissolved in water and concentrated to crystallization over concentrated sulfuric acid.

The anhydrous acid HPMo12 was prepared by heating the hydrated HPA at 403 K in an electric furnace for 4 h.

The HPW12·$3H_2O$ sample for structure analysis was prepared by heating the HPW12·13–29 hydrate at 433 K for 60 min. The water content of the product was calculated from its total weight loss after heating at 753 K for 60 min as 2.93 molecules H_2O per formula unit HPW12.

Rehydration treatment was carried out by exposure of the dehydrated samples to water vapor in a closed water filled desiccator for 12 h at room temperature.

The thermal experiments as well as XRD and TG measurements were performed under a dry air or nitrogen flow using 0.5–1 mm thin loosely packed powder samples in order to promote rapid desorption of water. Careful control of the atmosphere and temperature was necessary in order to obtain reproducibility in thermal experiments.

X-Ray diffraction

XRD powder patterns were recorded on a Siemens D-5000 theta/theta diffractometer using Cu-Kα radiation and a scintillation counter. The diffractometer was carefully adjusted and the correctness of the line positions was checked by calibration measurements using mica (NBS Standard Reference Material 675) as external standard. The measured line positions corresponded with the theoretical values within a tolerance window of $\pm 0.003^\circ$ 2θ. The programs Win-Index, Win-Metric and Win-Rietveld[14] were used for evaluation of the XRD diagrams and for the structure refinement. The calculation of the radial distribution function (RDF) was performed by Fourier transformation of the experimental intensity function using the PC program LAXS.[15]

High temperature XRD patterns were recorded *in situ* by means of a Bühler high temperature attachment equipped with a scintillation counter. In some experiments a position sensitive detector was used. The temperature was measured by means of a calibrated thermocouple mounted on the back of the platinum sample holder. This attachment controls the sample temperature during measurement within ± 2 K. Samples, ~ 0.5–1 mm thick, were heated under a dry air or nitrogen flow from room temperature to 873 K in steps of 20 K. The heating time was 1 h for each temperature.

Thermogravimetric analysis

TG was measured on a TA SDT 2960 thermal analyzer. Samples of *ca.* 5 mg in weight were heated in a platinum sample pan under a dry air or nitrogen flow up to 873 K at a constant heating rate of 10 K min^{-1}.

Results and discussion

Dehydration of $H_3PMo_{12}O_{40}$; the anhydride formation

Fig. 2 shows the high temperature X-ray diffraction patterns of the anhydrous acid heated under dry nitrogen flow at the indicated temperatures. At 653 K the stoichiometric anhydrous acid $H_3PMo_{12}O_{40}$ is present. At 673 K, 693 K and 713 K the XRD patterns still show some similarities with that of the anhydrous acid, but there are also distinct and significant differences. The loss of the constitutional water is accompanied by a progressive amorphization process. The XRD patterns are characterized by broad lines (halos) rather characteristic for amorphous than for crystalline materials. Moreover, all the diffraction lines of the anhydrous acid bearing indices (*hkl*) are strongly weakened or have disappeared completely, indicating that the three-dimensional periodicity of the rhombohedral structure has largely been lost. At 713 K the XRD pattern is dominated by the diffraction lines of β-MoO_3 (JCPDS 37-1445), which possess a perovskite like structure, and α-MoO_3.

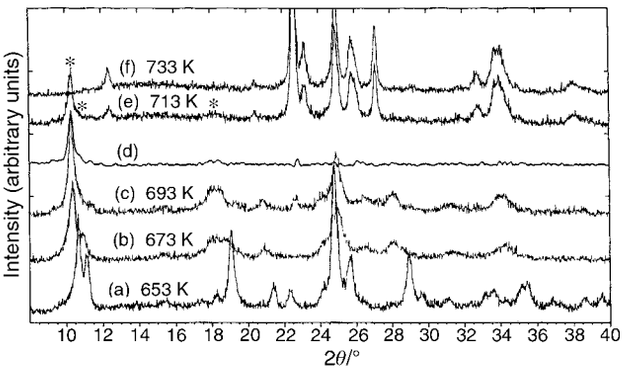

Fig. 2 High temperature XRD patterns of the anhydrous acid in the temperature range of the anhydride formation: (a) 653, (b) 673, (c) 693, (e) 713, (f) 733 K, (d) difference spectrum (e)−(f).

Owing to the progressive amorphization most of the diffraction lines shown in Fig. 2c disappeared at this temperature. The remaining few lines (marked with *) are represented in Fig. 2d as a difference spectrum, calculated by subtracting Fig. 2f from the spectrum shown in Fig. 2e. At 733 K the XRD pattern shows the diffraction lines of β-MoO_3 and of α-MoO_3. The water content of the samples a–f was calculated from the total weight loss at 753 K in separate experiments. Results are shown in Table 1.

According to Table 1 and to the presented XRD data the formation of the anhydride, the state for which the solid keeps constant weight, can be represented by the following scheme:

$$\underset{\text{(a)}}{H_3PMo_{12}O_{40}} \rightleftarrows \underset{\text{(b)}}{H_{0.17}PMo_{12}O_{38.585}} + 0.9H_2O \rightleftarrows$$

$$\underset{\text{(c)}}{(PMo_{12}O_{38.5})_n} + 0.6H_2O \rightarrow \underset{\text{(d)}}{(PMo_{12}O_{38.5})_n} + \beta\text{-}MoO_3 +$$

$$\alpha\text{-}MoO_3 \rightarrow \beta\text{-}MoO_3 + \underset{\text{(e)}}{\alpha\text{-}MoO_3}$$

Sample (b) still contains about 5.6% of the protons compared with the anhydrous acid. The samples (c), (e) and (f) are essentially free of water and represent, at least formally, anhydride states.

The chemical composition and properties of phase (c), formed above the temperature of the constitutional water loss (673 K) and before the formation of the molybdenum oxides (713 K), correspond to the common definition of a true acid anhydride in every respect: it is essentially free of water and the initial hydrated compounds with the complete amount of water of crystallization are restored by rehydration in a water saturated atmosphere.

In contrast, the MoO_3 phases formed in the temperature range between 713 K and 733 K do not represent true anhydride states with respect to the reversibility of the dehydration–rehydration process. The rehydration of sample (e) effects only a partial reconstruction into the hydrated HPA and the MoO_3 formed by dehydration at 733 K could not be rehydrated even by exposure to water vapor for 12 hours. Moreover, a precise lattice constant determination showed that the lattice parameters of the β-MoO_3 and α-MoO_3 phases differ slightly from those of the pure oxides. The MoO_3 phases probably represent solid solutions of phosphorus in molybdenum oxide[9] rather than a stoichiometric anhydride phase. Therefore, we will refer to phases (c) and (d) as the true anhydride in the following discussion.

Dehydration of HPVMo11·yH_2O shows very similar TG and XRD results, with the difference that the phase transformations occur at slightly lower temperatures. The phases observed in the dehydration process are isostructural with the corresponding HPMo12 structures.

Formation of $H_3PW_{12}O_{40}\cdot 3H_2O$

In contrast to HPMo12·yH_2O, the dehydration of HPW12·yH_2O takes place in two distinct steps with the formation of two distinct acid hydrates. The plateau between ~363 and 420 K in Fig. 1b corresponds to $6H_2O$ molecules per HPW12 formula unit. The high temperature XRD diagram (Fig. 3, 413 K) shows the cubic Keggin structure. The weight loss between ~420 K and 600 K corresponds to the release of the six molecules of water. However, as clearly indicated in the marked temperature window (c) in Fig. 1b, the release of the water of crystallization takes place in two separate steps. At about 473 K, after the loss of about 3.6 molecules of water, the dehydration curve decreases in slope and the dehydration process becomes slower. Because thermograms, at least in temperature ranges of rapid weight losses, do not represent equilibrium curves[6] the exact water content of a sample was determined in a separate isothermal experiment as 2.93 molecules H_2O per HPW12 formula unit and this sample was used for structure analysis. The question whether the dehydration temperature could be varied to control the formation of different hydrates of the general composition $(H_3O)_xH_{3-x}PMo_{12}O_{40}$ could be formed was not elucidated in detail.

Table 1 Water content of samples (a)–(f) from Fig. 2 after calcination at 753 K for 1 h

Temperature/K	H_2O *m/m*	Phase composition
653	1.487	$H_3PMo_{12}O_{40}$
673	0.2528	$H_{0.17}PMoO_{38.585}$
693	0.0	$(PMo_{12}O_{38.5})_n$
713	0.0	$(PMo_{12}O_{38.5})_n + \beta\text{-}MoO_3 + \alpha\text{-}MoO_3$
733	0.0	$\beta\text{-}MoO_3 + \alpha\text{-}MoO_3$

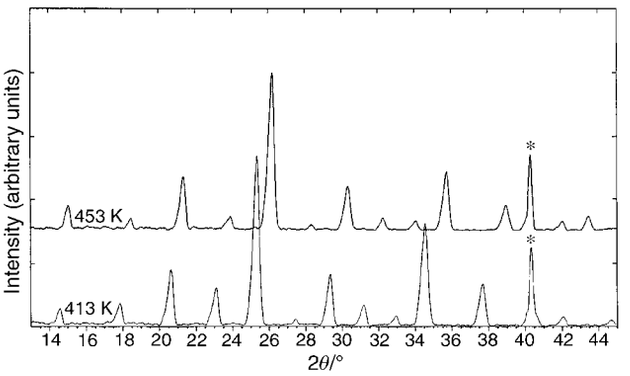

Fig. 3 High temperature XRD patterns of the dehydration of HPW12·yH_2O at 413 K and 453 K; * denote diffraction lines of the Pt/Rh sample holder.

In the temperature range between 420 K and 520 K in XRD a remarkable phenomenon occurs which was not mentioned in earlier reports. The lattice constant drops from 12.1666 to $a = 11.78$ Å and characteristic changes in the relative line intensities compared with the cubic hexahydrate are to seen (Fig. 3, 453 K). The structure of this novel trihydrate remains still cubic up to 523 K. Above this temperature the trihydrate decomposes into the anhydrous acid which is isostructural with the corresponding anhydrous HPMo12 HPA.

Because it seemed to us extremely unlikely that in spite of the numerous TG and XRD experiments the appearance of the trihydrate should never have been observed in former experiments we examined a great number of TG and XRD patterns published in the literature and found that both effects, the two step mechanism of the hexahydrate dehydration[11,16] as well as the sudden decrease in lattice constant,[6] are clearly indicated in some, but not all, papers. No publication was found for which both effects were described. We have found that careful control of the sample geometry, which in turn influences the local atmosphere in the vicinity of the particles, and of temperature are necessary in order to obtain reproducibility in thermal experiments. A detailed study on the relevance of the atmosphere for the decomposition temperature and for the structure of the thermal decomposition products is in progress and results will be published in a separate paper.

Structure determination of $H_3PMo_{12}O_{40}$

Unit cell determination. Our indexing of the observed diffraction pattern (Fig. 2a) led to a trigonal unit cell. Crystal data are presented in Table 3. Calculated and measured *d*-values and the integrated line intensities are reported in Table 2. The diffraction diagram shows only reflections for

Table 2 Measured and calculated *d*-values and intensities for the trigonal $H_3PMo_{12}O_{40}$, $a=15.8753$ Å, $c=20.7525$ Å

h k l	*d*(obs)	*d*(calc)	*I*(obs)	*I*(calc)
0 1 2	8.2802	8.2822	5510	5002
1 1 0, 2 −1 0	7.9359	7.9376	3216	3096
0 0 3	6.9147	6.9175	187	133
2 0 2	5.7306	5.7307	793	563
2 1 1, 3 −1 1	5.0410	5.0408	369	267
1 0 4	4.8541	4.8540	868	926
1 2 2, 3 −2 2	4.6450	4.6463	4368	4210
0 3 0	4.5837	4.5828	714	732
0 2 4	4.1407	4.1411	1465	1465
2 2 0, 0 1 5, 4 −2 0	3.9678	3.9688	1091	1184
0 3 3, 3 0 3	3.8210	3.8205	119	129
2 1 4	3.6715	3.6715	481	502
4 −1 2, 3 1 2	3.5792	3.5791	9469	9290
0 0 6	3.4588	3.4588	3572	3270
1 3 4	3.0723	3.0725	3360	3500
4 1 0	2.9998	3.0001	258	260
1 0 7	2.8982	2.8980	49	51
4 0 4	2.8654	2.8653	863	806
3 0 6, 0 3 6	2.7609	2.7607	210	245
3 2 4, 5 −2 4	2.6953	2.6951	615	591
5 0 2	2.6582	2.6579	1140	1188
2 2 6, 4 −2 6	2.6069	2.6075	359	479
0 1 8	2.5492	2.5491	1061	956
4 2 2, 6 −2 2	2.5209	2.5204	1609	1536
0 5 4	2.4292	2.4295	548	518
6 −5 2	2.4008	2.4022	209	149
2 4 4, 6 −4 4	2.3227	2.3232	563	618
1 4 6, 4 1 6	2.2661	2.2663	854	1000
5 1 4, 6 −1 4	2.2295	2.2296	307	221
3 1 8, 4 −1 8	2.1446	2.1448	279	259
3 3 6, 6 −3 6	2.1012	2.1015	399	219

planes with $-h+k+l=3n$ and for planes 000*l* and *hh*2*hl* only with $l=3n$ indicating rhombohedral symmetry and *R*3 or *R*3*m* as the most probable space groups. The corresponding rhombohedral cell has the parameters $a=11.48$ Å, $\alpha=87.46^\circ$ and $Z=2$.

Structure determination. The rhombohedral unit cell shows a conspicuous similarity to that of the structurally well described cubic ammonium salt[17] and other isostructural compounds. The lattice constants are nearly identical, $a_{rh}=11.48$ Å compared with 11.6878 Å of the cubic cell, and the rhombohedral angle of 87.46° lies near 90°. The trigonal set up of the cubic cell along the C_3 (111) axis leads to a hypothetical trigonal cell of dimensions $a=16.400$ Å, $c=20.09$ Å, compared with $a=15.875$ Å, $c=20.75$ Å for the rhombohedral cell of the anhydrous acid.

The atomic arrangements in the two structures can be compared in a one dimensional projection by RDF analysis as usual in the structural analysis of amorphous materials. The results of the RDF analysis of the cubic ammonium salt and of the anhydrous acid are shown in Fig. 4a and b. It shows that

Table 3 Crystal data for the anhydrous acid

Chemical formula	$H_3PMo_{12}O_{40}$
Formula weight	1825.214
Crystal system	Trigonal
Space group	
Unit cell dimensions:	
a/Å	15.875(6)
b/Å	15.875(6)
c/Å	20.752(10)
α/°	90
β/°	90
γ/°	120
V/Å^3	4528.16
Z	6
D_c/g cm^{-3}	4.0143

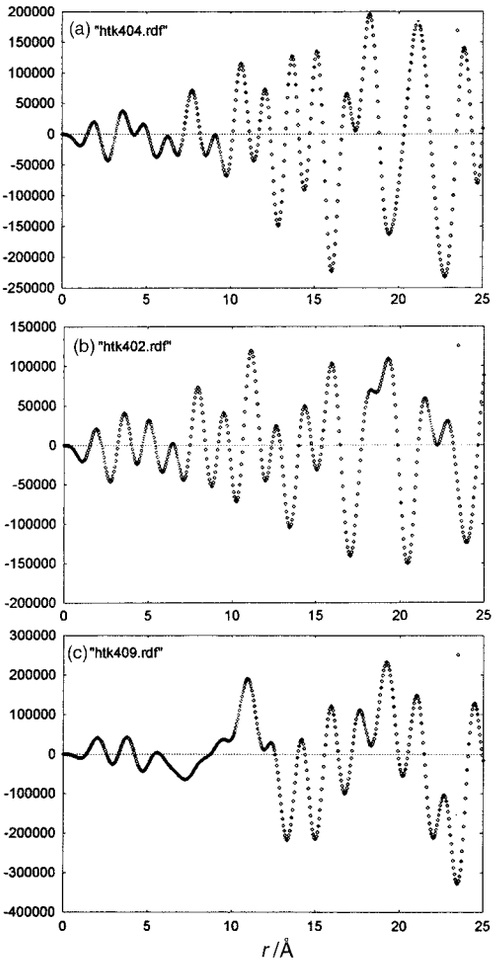

Fig. 4 RDFs of (a) NH_4PMo12, (b) anhydrous HPMo12 and (c) the anhydride phase.

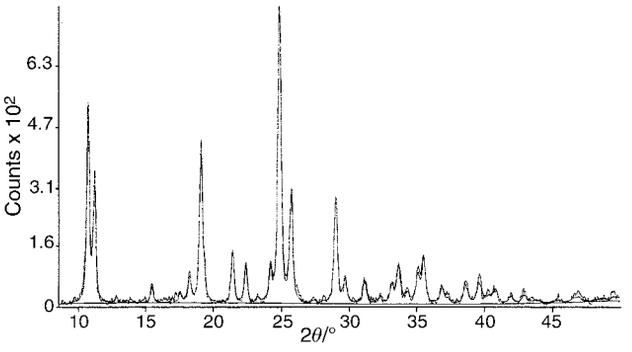

Fig. 5 Rietveld refinement plot of the trigonal $H_3PMo_{12}O_{40}$, observed (continuous line) and calculated (dotted line) XRD pattern; goodness of fit $S = R_{WP}/R_{EXP} = 1.24$.

the atomic radial distribution functions of the two HPAs are very similar suggesting a close structural relationship between the atomic arrangements in the two structures.

Therefore, the first set of fractional atomic co-ordinates for molybdenum, phosphorus and oxygen of the anhydrous acid was calculated from that of the cubic ammonium salt by transformation into the trigonal cell. These values were used as starting co-ordinates in the Rietveld structure refinement. The refinement was carried out in space group $R3H$. Compared with the starting orientation the progressive refinement of the atomic parameters led to a significant turn of the Keggin units round the (00*l*) cell axis and to a significant shortening of the interatomic distances between the polyanions along (*h*00). The result of the Rietveld refinement is shown in Fig. 5. The goodness of fit is $S = R_{WP}(0.162)/R_{EXP}(0.131) = 1.24$. The resulting fractional atomic co-ordinates of the P and Mo atoms are listed in Table 4, individual interatomic distances and angles are shown in Table 5. The three-dimensional arrangement of the Mo and P atoms is shown in Fig. 6. It can be seen from Fig. 6 that the structure of the Keggin units is preserved in the anhydrous state. However, due to the lowering of the point group symmetry from T_d in cubic salts to 3 in the trigonal anhydrous acid, the cubooctahedra are significantly distorted. In the structure of the cubic ammonium salts there are two distinct Mo–Mo distances.[17] A short distance of 3.41 Å within the Mo_3 triplets and a longer one of 3.72 Å between the Mo_3 triplets. The P–Mo distances are 3.54 Å. In different cubic HPA salts the above mentioned atomic distances vary between 3.25–3.42 Å within and 3.68–3.74 Å between the Mo_3 triplets. It can be seen from Table 5 that all distances and angles of the anhydrous acid are within reasonable limits and comparable with interatomic distances found in different Keggin type HPA structures.

The arrangement of the Mo atoms in the structure of the anhydrous acid is represented in Fig. 7 in a two dimensional projection along 00*l*. Compared with the cubic ammonium salt (Fig. 7a), the rotation of the Keggin molecules in the structure of the anhydrous acid round the (00*l*) cell axis is clearly indicated. Preliminary analysis of the interatomic distances and angles for geometrically favorable hydrogen bridging sites shows that the terminal OH groups probably form direct hydrogen bridges between the polyanions. The crystal structure of the anhydrous acid seems to be governed by Mo–O–H···O–Mo bridges formed by OH groups between the oxygen shells of the neighboring polyanions instead of hydrogen bonding by some molecules of water. Further details of the structure analysis and a detailed description of this new HPA structure will be published in a separate paper.

Table 4 Fractional atomic co-ordinates of the Mo and P atoms of trigonal $H_3PMo_{12}O_{40}$

Atom	*x*	*y*	*z*
P(1)	0.0000	0.0000	−0.9540(39)
P(2)	0.0000	0.0000	0.4100(41)
Mo(1)	−0.1199(13)	−0.1493(11)	0.5460(7)
Mo(2)	0.1962(12)	−0.0500(12)	−0.1015(13)
Mo(3)	0.2436(11)	0.2096(11)	−0.1029(8)
Mo(4)	0.0298(14)	−0.1040(14)	0.2796(7)
Mo(5)	−0.1052(14)	−0.1383(13)	0.0400(7)
Mo(6)	0.1940(11)	−0.0586(10)	0.4003(10)
Mo(7)	0.2349(12)	0.1945(12)	0.4100(12)
Mo(8)	0.0440(14)	−0.1090(14)	−0.2434(7)

Table 5 Significant interatomic distances (Å) and angles (°) for the anhydrous acid

P(1)–Mo(2)	3.600	P(1)–Mo(5)–Mo(2)	60.23, 94.93, 119.82
P(1)–Mo(3)	3.651	P(1)–Mo(59)–Mo(3)	65.75, 86.64, 125.05
P(1)–Mo(5)	3.461	P(1)–Mo(59)–Mo(5)	59.95
P(1)–Mo(8)	3.781	P(1)–Mo(5)–Mo(8)	119.09, 121.10, 178.25
Mo(3)–Mo(2)	3.8219	Mo(2)–Mo(3)–Mo(2)	121.36
	3.4199	Mo(3)–Mo(2)–Mo(3)	118.63
Mo(5)–Mo(5)	3.4578	Mo(5)–Mo(5)–Mo(5)	60
Mo(8)–Mo(8)	3.7756	Mo(8)–Mo(8)–Mo(8)	60
P(2)–Mo(1)	3.584	P(2)–Mo(4)–Mo(1)	117.37, 118.43, 177.71
P(2)–Mo(4)	3.344	P(2)–Mo(4)–Mo(4)	60.39
P(2)–Mo(7)	3.472	P(2)–Mo(4)–Mo(7)	57.3, 94.92, 117.03
P(2)–Mo(6)	3.661	P(4)–Mo(4)–Mo(6)	58.65, 84.54, 118.7
Mo(7)–Mo(6)	3.7615	Mo(7)–Mo(6)–Mo(7)	114.6
	3.3806	Mo(6)–Mo(7)–Mo(6)	124.76
Mo(1)–Mo(1)	3.787	Mo(1)–Mo(1)–Mo(1)	60
Mo(4)–Mo(4)	3.3635	Mo(4)–Mo(4)–Mo(4)	60

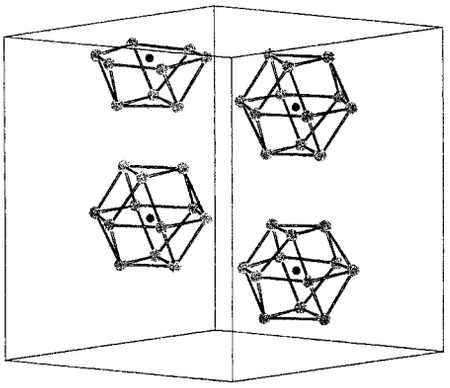

Fig. 6 Three-dimensional arrangement of the Keggin units in the structure of the anhydrous acid $H_3PMo_{12}O_{40}$. (Only three of the six cubooctahedrons are shown.)

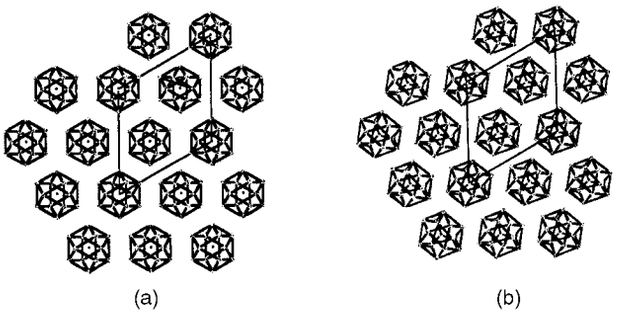

Fig. 7 Schematic polyhedral representation of the structures of (a) the cubic NH_4PMo12 salt and (b) trigonal HPMo12 viewed along the *c*-axis.

Structure of the acid anhydride

The XRD diagrams of the anhydride phases, represented in Fig. 2c and d, still show some similarities with that of the anhydrous acid, but there are also distinct and significant

differences. All the reflections from planes bearing indices (*hkl*) are considerably weakened or have disappeared indicating that the three dimensional periodicity of the rhombohedral structure has largely been lost during the release of the constitutional water. The trigonal unit cell of the anhydrous acid can not longer be applied for indexing the XRD pattern of the anhydride phase. The peaks in Fig. 2c and d represent noncrystalline diffraction maxima due to the frequent occurrence of particular atomic distances in a largely disordered material, rather than reflections by regular atomic planes according to the Bragg equation. Therefore RDF analysis of the experimental intensity function was performed in order to obtain information about the atomic arrangement in the anhydride structure. The resulting RDF, which gives the difference between the observed and the average atomic distribution, is shown in Fig. 4c. It shows several distinct atomic distances which are very similar to those in the structure of the rhombohedral acid (Fig. 4b). The distribution functions can be analyzed in terms of a number of intra- and intermolecular distances corresponding to different levels of order in the scattering material. First of all, it is possible to distinguish the atomic distances associated with the Keggin units. The peaks at ~2, ~3.7 and ~5 Å can be associated with the Mo–O and Mo–Mo distances inside the Keggin unit. The second level of order arises due to the aggregation of the Keggin units to form a crystal or an amorphous particle. The Keggin unit can be considered as a rigid sphere resulting from the compact packing of linked MoO_6 octahedra and its scattering function can be represented by its molecular scattering function in an approximate way. In the rhombohedral acid each Keggin anion is surrounded by eight others at a distance of about 11 Å. The most intense peak in the RDF at 11 Å can therefore satisfactorily be attributed to the separation between the centres of gravity of neighboring Keggin anions. A further level of organization arises when the Keggin units are ordered to form a three-dimensional periodic crystal. In this case, the statistically disordered intermolecular distances between the polyanions become ordered to form regular three-dimensional net planes which are characteristic for crystalline materials. Consequently, the peaks between 7 and 11 Å in the RDF of the rhombohedral acid must be assigned to the interatomic distances between the neighboring polyanions. In contrast, if the mutual orientation of the Keggin units is arbitrary no distinct intermediate distances are to be expected in the RDF. This disorder is reflected in the RDFs of the anhydride sample (d) by the missing or strongly weakened peaks between 7 and 11 Å. On the basis of the RDF analysis, it appears very likely that the structure of the Keggin units is preserved in the anhydride state. Moreover, the relative amplitude of the 11 Å peak has been found to be of the same order both in the anhydrous acid and in the corresponding anhydride indicating that the number of neighboring polyions must be of the same order. These results allow us to design a three dimensional model of the anhydride structure. As a result of the release of the constitutional water, the Keggin units, on the molecular level of the $PMo_{12}O_{40}$ complexes, are expected to be alternately positively and negatively charged according to the equation

$$2H_3PMo_{12}O_{40} \equiv PMo_{12}O_{39}^{-} + PMo_{12}O_{38}^{+} + 3H_2O$$

Similarly to the three dimensional arrangement of the polyanions in the rhombohedral structure, each polyion is surrounded by 8 others of opposite charge. This arrangement is characteristic for ionic crystals of the CsCl type. The high amplitude of the peaks at 11 Å and around 20 Å in the RDFs shows that the wide range order of the Keggin units is, at least in part, preserved in the anhydride state. The anhydride structure, therefore, can be considered as a highly disordered pseudocrystalline phase with respect to the inter and intramolecular distances and also to the three-dimensional geometrical arrangement of the Keggin molecules.

Structure of $H_3PW_{12}O_{40}\cdot 3H_2O$

The XRD patterns of the hexahydrate and of the new trihydrate are shown in Fig. 3. The similarities between the two XRD patterns are obvious indicating two closely related but clearly distinguishable structures. The loss of $3H_2O$ molecules is accompanied by a large decrease in the lattice constant from $a=12.506$ Å for the hexahydrate[18] to $a=11.75$ Å for the new trihydrate and by distinct changes in the relative line intensities.

The Rietveld refinement was started using the atomic co-ordinates of the W and the framework O atoms of the hexahydrate. The extra framework oxygen atoms were first placed in the crystallographic positions as found in the hexahydrate structure and were refined with retention of the $H_5O_2^+$ ion geometry and the H-bonding angles to the neighboring Keggin anions. The occupancy factor of the cations was set to 0.25 compared to 0.5 in the hexahydrate. The refinement led to a Bragg *R*-factor of 12.243% and the agreement between the observed and calculated intensity patterns was unsatisfactory. A significant improvement of the *R* factor could, however, be achieved by refinement of the positional parameters and occupancy factors of the extra framework oxygen atoms. The progressive refinement led to a significant shift of the oxygen atoms from the x, $\frac{1}{4}$, $\frac{3}{4}$ positions into the regular cationic positions $\frac{1}{4}$, $\frac{3}{4}$, $\frac{3}{4}$ accompanied by a significant lowering of the Bragg *R*-factor from 12.243% to 4.37%. The goodness of fit is excellent, with $S=R_{WP}/R_{EXP}=1.13$. The result of Rietveld refinement is shown in Fig. 8, the atomic co-ordinates are listed in Table 6.

Although the crystallographic positions of the H atoms could not be found from the X-ray powder data the presence of $H_5O_2^+$ ions in the structure of the new trihydrate is rather unlikely and the assumption of H_3O^+ ions appears to be more reasonable in view of the measured lattice constants and of recent literature on the dehydration mechanism of $H_5O_2^+$ ions.[19,20]

On the one hand, in the hexahydrate structure the polyanions are linked by nearly planar $H_5O_2^+$ dioxonium cations. The proton is symmetrically situated between the two water molecules with an O···H···O distance of 2.37 Å which is one of the shortest ever observed involving O atoms. The minimum bond length for a symmetrical O···H···O bond can be calculated from the Pauling equation $d_n=0.60\times\log n$[21] to 2.3–2.36 Å compared with 2.37 Å in the dioxonium cation. Analysis of the interatomic distances in the trihydrate structure showed that the shortening of the lattice constant from 12.5 Å for the hexahydrate to 11.73 Å for the trihydrate would lead, under maintenance of the favorable geometrical situation for

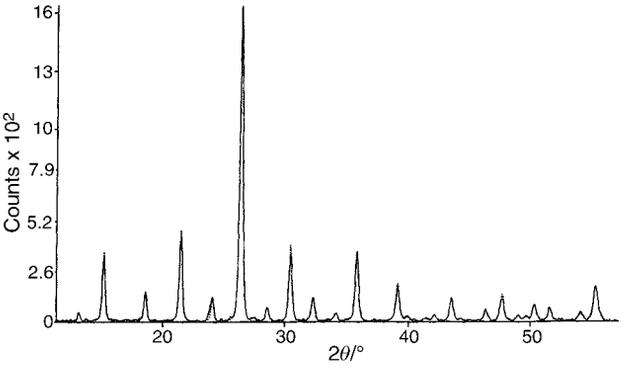

Fig. 8 Rietveld refinement plot of $H_3PW_{12}O_{40}\cdot 3H_2O$, observed (continuous line) and calculated (dotted line) XRD pattern; goodness of fit $S=R_{WP}/R_{EXP}=1.13$.

Table 6 Fractional atomic co-ordinates of the W, P and O atoms of $H_3PW_{12}O_{40}\cdot 3H_2O$

Atom	*x*	*y*	*z*
P	0.75	0.75	0.75
W	0.7579(2)	0.9636(2)	0.9636(1)
O(1)	0.8226(8)	0.8226(8)	0.8226(8)
O(2)	0.6453(11)	0.8527(11)	1.0133(12)
O(3)	0.8687(6)	0.8687(6)	1.0462(11)
O(4)	0.7412(9)	1.0629(7)	1.0629(7)
O(W)	0.75	1.25	1.25

OH bridges, to an exceptionally short O···H···O distance of only 2.22 Å which, however, appears unrealistic.

On the other hand, IR and Raman spectroscopic studies of $HPW12\cdot yH_2O$ at 473 K support the formation of H_3O^+ cations with increasing degree of dehydration. The loss of water from the hexahydrate follows the pathway

$$H_5O_2^+ \leftrightharpoons H_3O^+ + H_2O \leftrightharpoons H^+ + H_2O$$

The equilibrium is displaced towards right side with decreasing water content.[20] It was shown that the loss of water during dehydration of the hexahydrate is followed by an increase in H_3O^+ ion concentration. Therefore, it appears very likely that in the trihydrate structure H_3O^+ cations are present. The molecular formula for the new trihydrate should therefore be written as $(H_3O^+)_3(PW_{12}O_{40})$ and thus this acid represents the missing hydrate according to the pathway of the $H_5O_2^+$ ion dehydration scheme.

Summary

The successful structural characterization of the $PW12\cdot 3H_2O$ HPA, of the anhydrous acid HPMo12 and of the corresponding anhydride $Mo_{12}O_{38.5}$ from XRD powder data provides a complete insight into the structures of dehydrated HPAs which are involved in catalytic reactions.

The formulation of the new trihydrate as $(H_3O^+)_3(PW_{12}O_{40})$ is very likely and further experiments to confirm this structure are in progress.

Our structural model of the anhydride structure can explain some of the controversial results published in the literature. The release of constitutional water occurs in a very small temperature window between 673 K and 713 K. It seems to us very likely that owing to slightly different experimental conditions the structural transformation of the anhydrous acid into the anhydride can lead to the formation of different intermediate structures having different degrees of order and consequently different XRD patterns.

No great change in crystal structure accompanies the release of the crystal and constitutional water from the acid hexahydrate towards the anhydride. The three dimensional arrangement of the Keggin units remains nearly unchanged, only their mutual orientation changes with the water content. The structures of the higher hydrates as well as of the anhydrous acids and anhydrides are governed by the well known electrostatic radius ratio principles observed for extended ionic crystals and by hydrogen bonding between the polyanions.

References

1 N. Mizuno and M. Misono, *Chem. Rev.*, 1998, **98**, 199.
2 M. Misono, *Catal. Rev. Sci. Eng.*, 1987, **29**, 269.
3 G. Ya. Popova and T. V. Andrushkevich, *Kinet. Catal.*, 1994, **35**, 120.
4 Th. Ilkenhans, B. Herzog, Th. Brown and R. Schlögl, *J. Catal.*, 1995, **153**, 275.
5 C. Rocchiccioli-Deltcheff, A. Aouissi, M. M. Bettahar, S. Launay and M. Fournier, *J. Catal.*, 1996, **164**, 16.
6 M. Fournier, C. Feumi-Jantou, C. Rabia, G. Hervé and S. Launay, *J. Mater. Chem.*, 1992, **2**, 971.
7 S. Albonetti, F. Cavani, F. Trifirò, M. Gazzano, M. Koutyrev, F. C. Aissi, A. Aboukais and M. Guelton, *J. Catal.*, 1994, **146**, 491.
8 A. Bielanski, A. Malecka and K. Kubelkova, *J. Chem. Soc., Faraday Trans. 1*, 1989, **85**, 2847.
9 V. M. Bondareva, T. V. Andrushkevich, R. I. Maximovskaya, L. M. Plyasova, A. V. Ziborov, G. S. Litvak and L. G. Detuseva, *Kinet. Catal.*, 1994, **35**, 114.
10 H. G. Jerschkewitz, A. Alsdorf, H. Fichtner, W. Hanke and G. Öhlmann, *Z. Anorg. Chem.*, 1985, **526**, 73.
11 E. Payen, S. Kasztelan and J. B. Moffat, *J. Chem. Soc., Faraday Trans.*, 1992, **88**, 2263.
12 Ai Chau Dieu, P. Reich, E. Schreier, H. G. Jerschkewitz and G. Öhlmann, *Z. Anorg. Chem.*, 1985, **526**, 86.
13 G. A. Tsigdinos and C. J. Hallada, *Inorg. Chem.*, 1968, **7**, 437.
14 Sigma-C GmbH, München, 1991.
15 LAXS, Fortran IV Program, Version 19940714, 1994.
16 H. Hayashi and J. B. Moffat, *J. Catal.*, 1982, **77**, 473.
17 J. C. A. Boeyens, G. J. McDougal and J. Van R. Smit, *J. Solid State Chem.*, 1976, **18**, 191.
18 G. M. Brown, M. R. Noe-Spirlet, W. R. Busing and H. A. Levy, *Acta Crystallogr., Sect. B.*, 1977, **33**, 1038.
19 G. B. McGarway and J. B. Moffat, *J. Catal.*, 1991, **130**, 483.
20 U. Mioc, M. Davidovic, N. Tjapkin, Ph. Colomban and A. Novak, *Solid State Ionics*, 1991, **46**, 103.
21 L. Pauling, *J. Am. Chem. Soc.*, 1947, **69**, 542.